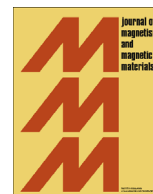Contents lists available at ScienceDirect

Journal of Magnetism and Magnetic Materials

journal homepage: www.elsevier.com/locate/jmmm

Polaronic ferromagnetic behavior in ClO_4^- doped poly(3-hexylthiophene) at room temperature

F.R. de Paula [a,c], D. Schiavo [b,c], E.C. Pereira [b,c,**], A.J.A. de Oliveira [a,c,*]

[a] Departamento de Física, Universidade Federal de São Carlos, CP 676, 13565-905 São Carlos, SP, Brazil
[b] Departamento de Química, Universidade Federal de São Carlos, CP 676, 13565-905 São Carlos, SP, Brazil
[c] Agilent Technologies, São Paulo, SP, Brazil

ARTICLE INFO

ABSTRACT

The magnetic properties of pressed pellets of ClO_4^- partially doped poly(3-hexylthiophene) have been investigated in the range from 5 to 300 K and a ferromagnetic phase was observed at room temperature. This behavior was associated to polaron interaction because the saturation magnetization, remanent magnetization, and coercive field, change with the reversible potential that modulates the doping level of the samples. This effect is a consequence of the Nernst potential describes the ratio among reduced sites, polarons and bipolarons in the sample. The results also show that the ferromagnetic phase vanishes when the samples undergo a thermal annealing or are stored under atmospheric conditions for a long period of time. The absence of contaminants such as Co, Fe and Ni was determined using inductively coupled plasma tandem mass spectrometry with ppb resolution. These results support that the ferromagnetic behavior observed in samples is intrinsic.

1. Introduction

The discovery of conducting polymers in the 1970s was one of the greatest revolutions in material science once it led to a new generation of electronic and optical devices [1–5]. One important property of these materials is the possibility of controlling the doping level, and as a consequence the electric conductivity. These systems are low dimensional compounds with linear π-conjugated bonds, and subjected to Peierls distortion [6]. Consequently, electron–phonon interaction and electron–electron correlation could result in the localization of π-electron along the conjugated backbone, and, in the case of nondegenerate ground state, leading to the formation of charged $\pm(e)$ spin polarons. The interaction between two polarons, under certain conditions, results in bipolarons with charge $\pm(2e)$ and spin 0. Due to a large interest on these characteristics, many works have investigated the magnetic behavior of such polymers [7–21]. Unlike conventional magnetic materials, which always involve spins of either d or f electrons, in

π-conjugated polymers p-electrons play an essential role in this property [9]. It arises from the intrinsic spin of unpaired electrons, which are introduced in the polymers through chemical or electrochemical oxidation (or reduction). Then, the mutual magnetic interaction between spins, either intrachain and/or interchain, could result in a ferromagnetic or antiferromagnetic phases [15].

Over the last few years, our group has systematically investigated the magnetic properties of conducting polymers, in particular in pellets of partially ClO_4^- doped poly(3-methylthiophene). Since the first observation in 2001 [11], we have studied different variables that influence the material magnetic properties present in different portions one of each is ferromagnetism at room temperature [13–17]. Recently, Vandeleene et al. [18,19] have also reported ferromagnetic phase in poly(3-alkylthiophene) in its neutral state and the influence of the substituent (alkyl, alkoxy, thioalkyl), and the regioregularity on the magnetic properties. The researchers observed the appearance of ferromagnetic phase at low temperature and superparamagnetic one at room temperature. In the case of our previous results, we have observed that the ferromagnetism depends substantially on the oxidation state and the applied pressure used to prepare the pellet [12,13].

In this work we present a systematic investigation of ferromagnetic phase in samples of pressed pellets of poly(3-hexylthiophene) partially doped with ClO_4^- in the temperature range from 5 to 300 K and discuss the origin of such behavior. The intrinsic

* Corresponding author at: Departamento de Física, Universidade Federal de São Carlos, CP 676, 13565-905 São Carlos, SP, Brazil.
** Principal corresponding author at: Departamento de Química, Universidade Federal de São Carlos, CP 676, 13565-905 São Carlos, SP, Brazil.
E-mail addresses: depaula@ymail.com (F.R. de Paula),
danischiavo@yahoo.com.br (D. Schiavo), decp@ufscar.br (E.C. Pereira),
adilson@df.ufscar.br (A.J.A. de Oliveira).

feature of this magnetic phase is found by studying the thermal and temporal stability of the samples as well as elemental analysis. Our results show that the magnetic behavior of samples is intrinsic.

2. Experimental details

The samples of poly(3-hexylthiophene) (P3HT) were electrochemically synthesized at 298 K using a constant potential of 1.60 V (referred to a quasi-reference silver electrode) and 0.2 M 3-hexylthiophene in acetonitrile. As supporting electrolyte, 0.1 M $LiClO_4$ was used. Previous works [14,17] have shown that the addition of a small amount of water to acetonitrile enhances the magnetic properties and leads to reproducible data. Therefore, an optimized amount of water, 0.2×10^{-3} M, was added to the solution. The synthesis was performed in a dry box filled with argon, to inhibit the contamination of the solution by moisture, and polymerization was performed using a total charge of 40 C. After the synthesis, the open circuit potential (in this case, a revisible one) of the polymer (E_{oc}) was of 1.08 V, which is characteristic of a sample in its oxidized state. The solution was changed twice in order to remove the soluble oligomers; afterwards, the samples were partially reduced, using small potential steps, in an acetonitrile solution with 0.1 M $LiClO_4$ until different values of E_{oc} were reached. This procedure is necessary since at high doping levels, polarons are unstable with respect to the pairing of their spin which leads to the formation of double charged spinless bipolarons. After the electrochemical reduction, the samples were removed from the Pt electrode using a glass spatula and were enclosed in a silicone die and isostatically pressed using 570 bar. This protocol for sample synthesis was established in a previous paper [12].

Different samples were prepared using the same procedure but changing the storage process before the magnetic characterization. In order to investigate the intrinsic nature of the magnetic behavior, Sample A was reduced to $E_{oc} = 0.80$ V and stored in air. For the same purpose, Sample B, prepared under the same conditions, was encapsulated in a quartz tube, evacuated and sealed. Before magnetic characterization, Sample B was placed in an oven at 400 K for 12 h. In order to study the thermal and external field effect on the magnetic properties, Sample C was also reduced until $E_{oc} = 0.80$ V and was stored under vacuum and protected from the light. To investigate the mechanism of the magnetic behavior, a set of samples reduced to different values of E_{oc} were studied.

To investigate the possibility of ferromagnetic contamination of the samples, a sample mass 10 mg was accurately weighed and digested with ultrapure nitric acid prepared using a sub-boiling apparatus (DuoPur, Milestone, Sorisole, Italy) and hydrogen peroxide. Digestion was carried out in a PFA closed vessel in a cavity microwave oven (Ethos model 1600, Milestone). All strategies were performed for avoiding contaminations and all vessels were decontaminated using nitric acid solution. A microwave-assisted heating program was performed with the reagents but without adding any sample just for cleaning the digestion vessels. Determinations of Co, Fe, and Ni were done using an inductively coupled plasma tandem mass spectrometer (ICP-MS/MS, Agilent 8800, Tokyo, Japan). The ICP-MS/MS was operated in MS/MS mass shifting mode to solve any spectral interferences and elements were determined using respective mass/charge ratios for their oxides formed in the octopole reaction system. Limits of detection for all three analytes were in sub-ppb range and all determined concentrations were below these values. Considering mass and volume ratios for sample digestion, final concentrations of Co, Fe, and Ni in the sample were lower than 0.010, 4.3, and 0.30 μg/g, respectively. Considering the detection

limit described in the previous line, it is important to stress out that no contamination was detected for any of the above elements.

Magnetization measurements were performed as a function of applied magnetic field at 5 K and 300 K ($M \times H$) using a Quantum Design SQUID magnetometer model MPMS-5S. Magnetization as a function of temperature measurements followed three different procedures: (i) the samples were cooled at zero field until 5 K, then the field is applied and the data were collected during the sample heat from 5 to 300 K. This procedure is called zero field cooling (ZFC). (ii) The data were measured during cooling (field cooling, FC) from 300 to 5 K. (iii) Spontaneous magnetization was measured after cooling down the sample without any applied magnetic field from 300 K to 5 K. After stabilizing temperature, the sample was submitted to a magnetic field of 50 kOe for 10 min and then removed. The magnetic moment was measured by increasing the temperature at constant rate (2 K/min) up to 300 K. In all samples, the diamagnetic contribution was observed as a linear behavior at high magnetic fields at 300 K and subtracted of the data by a linear fitting.

3. Results and discussion

First of all, it is important to eliminate the possibility that the ferromagnetic properties here observed are related with ferromagnetic contamination. This point has also been discussed in previous papers where atomic absorption spectroscopy in graphite furnace was used and no metallic contamination was detected in the samples [14,15]. In the present case, we carried out new inductively coupled plasma tandem mass spectrometer measurements, and, as described in the experimental section, no contamination of Fe, Co or Ni was detected, considering the detection limit of the measurements which were 4.3, 0.010, and 0.30 μg/g, respectively. Besides we proposed here a new set of magnetic experiments to assure the intrinsic magnetic behavior of the samples. In Fig. 1, the magnetization (M) as a function of applied magnetic field (H) for Sample A at 300 K is presented just after synthesis (circle), 30 (triangle) and 70 days (square) later. From Fig. 1 it is easy to observe that besides the decrease in the saturation magnetization (M_S), the coercive field (H_C) and remanent magnetization (M_R) disappear for the sample store for 70 days. Besides, the diamagnetic contribution remains constant, which is an indication that this part of the signal is related to the polymeric backbone itself. One explanation for this result is that aging time could partially reduce the material once the redox potential of the polymer is higher than the water/oxygen redox pair [22–24]. This is an evidence of two important points: (i) the
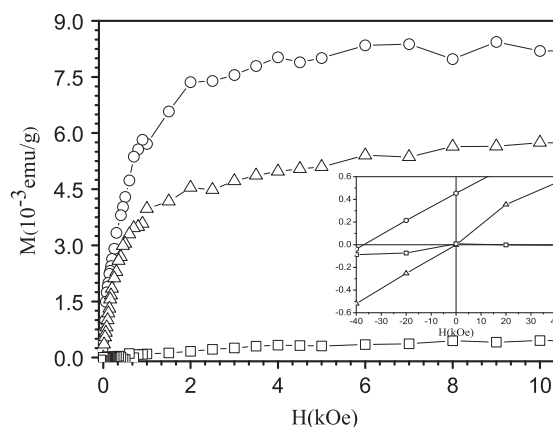

Fig. 1. Magnetization as a function of the magnetic field at 300 K; taken just after synthesis (circle) and the same sample measured 30 (triangle) and 70 days (square) later. Inset shows details of magnetization at low field.
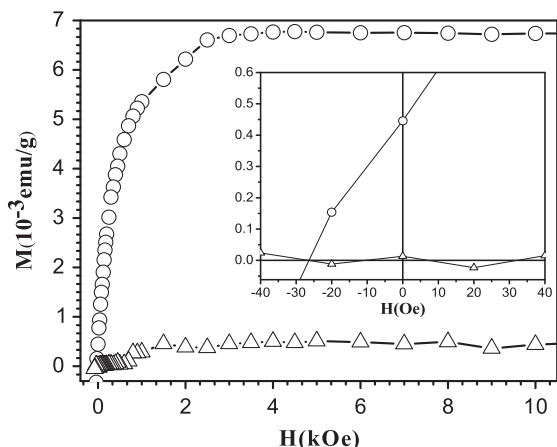
Fig. 2. Magnetization as a function of the applied magnetic field at 300 K; taken just after synthesis (circle) and after annealing at 400 K for 12 h (triangle). Inset shows an amplification of the portion central of the curve.

magnetic properties are intrinsic and (ii) this behavior is related to the doping level of the polymer.

To support the intrinsic nature of the ferromagnetic phase, the magnetization measurements as a function of applied magnetic field in Sample B were performed in two different conditions: just after synthesis and after annealing at 400 K for 12 h. Fig. 2 shows that M_S decreases and M_R and H_c vanish due to the annealing. The annealing of the samples led to chain bond degradation and, as a consequence, the electronic defects were also destroyed [20,24]. Furthermore, the temperature of 400 K is very low to promote any phase transformation in the majority of possible contaminants such as metal compound particles of Fe, Ni or Co. If any contaminant was responsible for the magnetic moments measured in the sample, their trace must continue to be observed.

The results presented in Figs. 1 and 2 support the fact that aging and annealing influence only the charged defect of the polymers, i.e., the polarons and/or bipolarons. In both situations, annealing and aging, the amount of defects is decreased and then the magnetic moments decrease too.

Then, we start to investigate the relationship of the doping level of the polymer and its magnetic properties. Fig. 3 presents M_S and M_R as a function of the reversible potential (E_{oc}) performed at 300 K and 5 K, i.e., we are looking for a correlation of the magnetic moments in the sample with the amount of polarons or bipolarons. It is well described in the literature that in the reduced state, i.e., for low E_{oc} values, the sample has a small density of charge carriers (polarons). In this case, from Fig. 3, it is also observed that M_S and M_R also present small values. When the polymer is in an intermediate oxidized state, M_S and M_R exhibit maximum value at 0.82 V. For higher open circuit potentials, M_S and M_R decrease again and vanish at 1.08 V. One explanation for such decrease is that, as E_{oc} increases, the polarons recombine into spinless bipolarons, and, as a consequence, there is not any unpaired spin interaction.

In previous works it was stated that the nature of ferromagnetic phase in partially doped conducting polymers is associated with the interaction between polarons [14,15]. It is important to stress that, as demonstrated here, it was possible to control polarons concentration by partially electrochemically reducing the samples using small potential steps, as described in the experimental section. For conducting polymers, the open circuit potential is a reversible one that follows Nernst equation and which is related to the ratio of the amount of oxidized and reduced sites. If a redox reaction follows Nernst equation, it means that it is a reversible one, i.e., the anodic and cathodic reactions are the same. Therefore, for conducting polymers, it means that E_{oc} values

are a ratio between the oxidized (Ox_{site}) and reduced (Re_{site}) sites. On condition of the samples synthesis, there are three different species, which react in the following equation:

$$Re_{site} \leftrightarrow P_{site} \leftrightarrow B_{site} \qquad (1)$$

where P_{site} and B_{site} are polarons and bipolarons, respectively. Re_{site} can be reversibly converted into polarons, as well as polarons can be reversibly converted into bipolarons. Therefore, for the sample with smallest E_{oc} shown in Fig. 3 there is only a small density of polarons. This is an indication that the sample was not in the most reduced state, what is reasonable since the samples are prepared in the oxidized state and step-by-step partially reduced to different E_{oc} values. Once the samples have a high electronic resistance as the reduction process is near from the most reduced state, there are capacitive current and shrinkage of the polymer chains that made very hard to obtain a complete reduced electronic defect-free sample.

When the E_{oc} value increases, it is observed that M_S and M_R rise until a maximum value at $E_{oc} = 0.82$ V. In this condition there is the conversion of Re_{site} into polaron defects. In fact, there is a competition between different processes: if the distance between two polarons is high enough there is no magnetic coupling between the polarons; as a consequence, the magnetic response when applying a magnetic field is a paramagnetic behavior. If the polaron population is very high, they are converted into bipolarons, and as a result, M_S and M_R decrease, as shown in Fig. 3. On the other hand, when the polaron population increases, the average distance decreases and the emergence of ferromagnetic interactions is observed. Then, an explanation for the ferromagnetic interaction of the polarons could be related to polaron interaction at different chains of the polymer which cannot be converted to bipolarons. This proposition is schematically represented in Fig. 4. Besides, it is important to highlight, in Fig. 3, that both curves, saturation and remanent magnetization ones, presented an asymmetric behavior for the slope of increase and decrease. This characteristic is also expected because the process of creation of polarons from Re_{site} and their destruction to form bipolarons are different.

For better understanding of magnetic behavior due to polarons, the analysis of the magnetization as a function of applied magnetic field ($M \times H$) at 5 K and 300 K shows the characteristics of interaction between two polarons. In Fig. 5 we present $M \times H$ measurement at 300 K (circle) and at 5 K (triangle) for Sample C. In this sample, the curve at 300 K exhibits the saturation magnetization (8.6×10^{-3} emu g^{-1}) at 5 kOe. In the inset, it is possible to identify a remanent magnetization of 0.45×10^{-3} emu g^{-1} and the coercive field of 40 Oe. The experiment performed at 5 K (triangle), with the same sample, shows that the ferromagnetic behavior is superimposed to a paramagnetic contribution. In the inset, it is observed that the $M_R = 0.94 \times 10^{-3}$ emu g^{-1} and a coercive field of 80 Oe. It is important to emphasize that, at this temperature, considering the maximum applied magnetic field used, the curve does not exhibit a significant diamagnetic contribution, which is reasonable because this contribution is negligible compared to the paramagnetic and ferromagnetic ones.

The curves shown in Fig. 5, from a point of view of magnetic behavior, lead to the conclusion that the sample presents a polymorphic behavior, with different magnetic portions. This hypothesis arises from the fact that the paramagnetic contribution is more important at low temperature compared to the ferromagnetic one. Because there is only one magnetic phase, a transition from the ferromagnetic to the paramagnetic is expected as the temperature is increased, and the reversed behavior is observed in Fig. 5. One explanation for the strong paramagnetic contribution is associated to non-interacting polarons as proposed elsewhere [15]. In order to estimate the paramagnetic contribution, at 5 K,
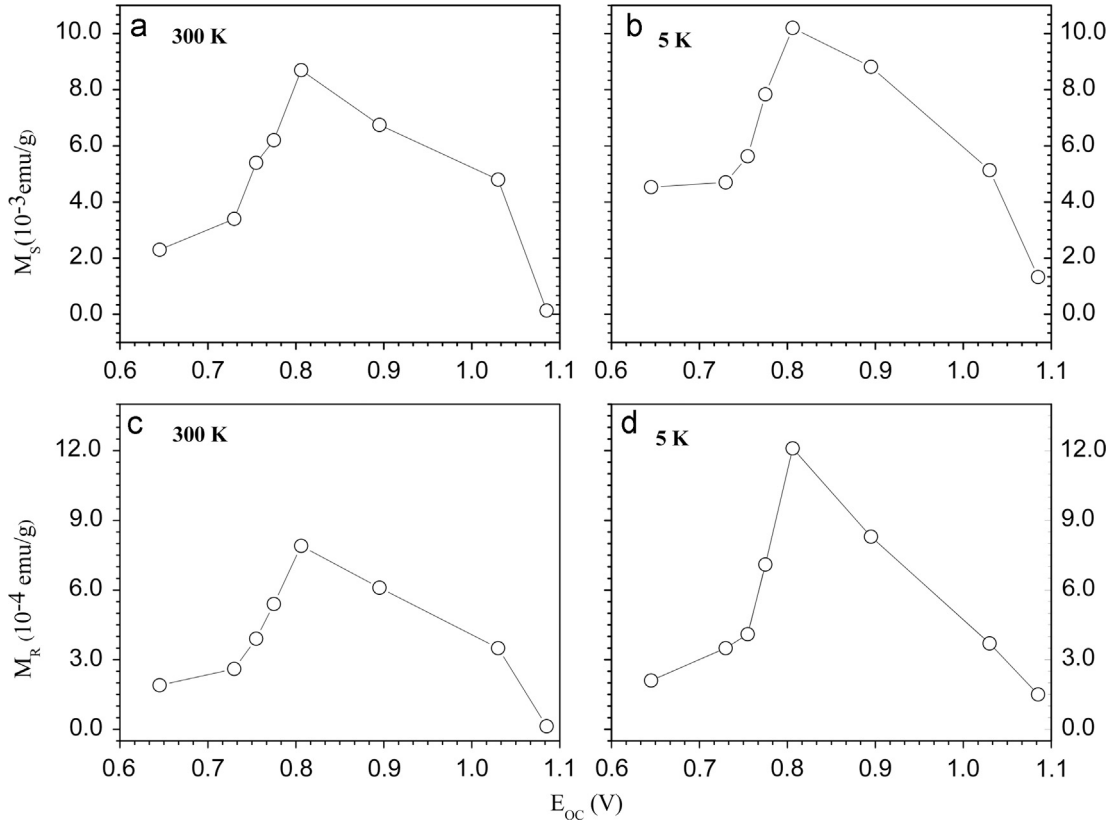
Fig. 3. Saturation (M_S) and remanent (M_R) magnetization as a function reduction potential (E_{oc}). (a) and (c) at 300 K and (b) and (d) at 5 K.
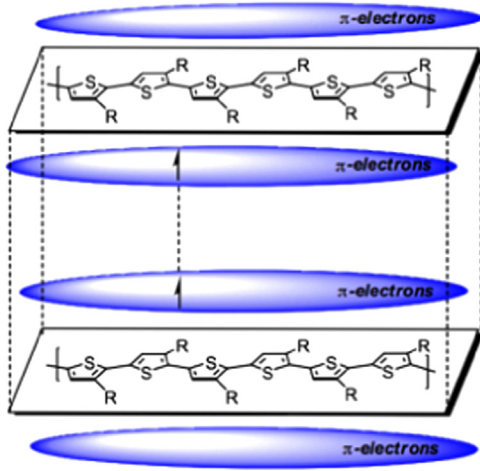

Fig. 4. Schematic representation of interchain polaron–polaron interaction.
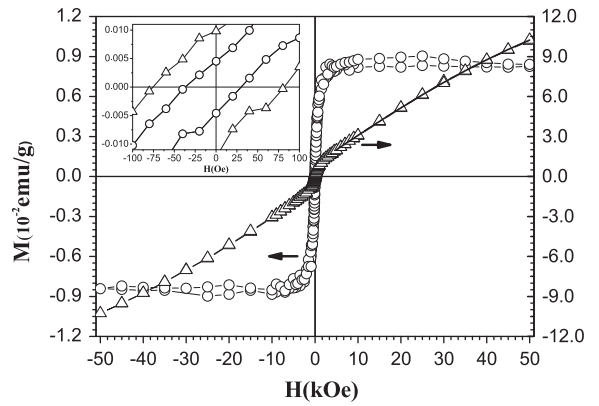

Fig. 5. Curve magnetization as a function of magnetic field at 5 K (triangle) and 300 K (circle) without the diamagnetic contribution. In curve at 5 K the solid line represents the fitting with expression $M(H) = M_1 + M_0 \tanh(\alpha H)$ for $H > 5$ kOe. Inset shows details of ferromagnetic hysteresis at 5 K and 300 K.

the Brillouin function is used as follows:

$$M = Ng\mu_B J B_J(\alpha H) \tag{2}$$

where $\alpha = \mu_B/k_B T$, H is the magnetic field, μ_B the Bohr magneton, k_B the Boltzmann constant, g the gyromagnetic constant of electron and B_J the Brillouin function given by

$$B_J(\alpha H) = \frac{1}{J}\left[\left(J+\frac{1}{2}\right)\coth\left(J+\frac{1}{2}\right)\alpha H - \frac{1}{2}\coth\left(\frac{\alpha H}{2}\right)\right] \tag{3}$$

If we consider that magnetic moments are associated with polarons with spin 1/2 ($J=1/2$) and $g \approx 2$, then Eq. (2) can be simplified as

$$M(H) = M_0 \tanh(\alpha H) \tag{4}$$

with

$$M_0 = N\mu_B \tag{5}$$

where M_0 is the paramagnetic saturation magnetization. A new parameter, M_1, was introduced in the equation to describe the magnetization saturation of the ferromagnetic portion. The final equation obtained is given by

$$M(H) = M_1 + M_0 \tanh(\alpha H) \tag{6}$$

From Fig. 5, fitting Eq. (6) to the curve measured at 5 K, the calculated parameters are $M_0 = 160.0 \times 10^{-3}$ emu g^{-1}, $M_1 = 8.6 \times 10^{-3}$ emu g^{-1}. As expected, M_1 values match the maximum values presented in Fig. 3b. For those partially reduced samples, the bipolarons concentration decreases, leading to the formation of polarons. Therefore, depending on the concentration of
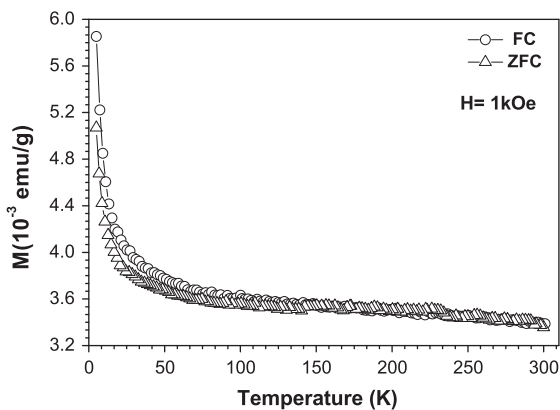
Fig. 6. Magnetization as a function of temperature: ZFC (circle) and FC (triangle) of sample C with applied magnetic field at 1 kOe.
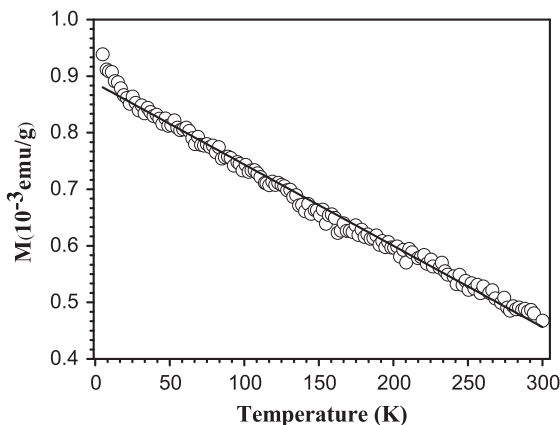

Fig. 7. Spontaneous magnetization as a function of temperature for sample C cooled without a field from 300 to 5 K. After this a magnetic field of 50 kOe was applied for 10 min and removed and increases temperature 2 K/min.

polarons, they can interact with polarons at different chains forming ferromagnetic regions, while others that interact weakly in the same chain could be responsible for the paramagnetic contribution of the sample.

The paramagnetic behavior shown in Fig. 5 at 5 K is more evident in Fig. 6 that presents the magnetization as a function of the temperature for sample C at 1 kOe, using ZFC/FC protocol. The magnetization decreases when the temperature increases, though there are different behaviors. First, at low temperature, the sample shows the typical paramagnetic behavior whereas after 150 K, its decrease resembles a ferromagnetic one, supporting the polymorphic behavior of the samples. Further evidence is the difference between curves ZFC / FC, as for temperatures below 150 K show a thermomagnetic hysteresis

Finally, the intrinsic ferromagnetic behavior of the samples was also observed in measurements of spontaneous magnetization as a function of the temperature (Fig. 7). In this case, the sample was cooled from 300 to 5 K without any applied field. At 5 K a magnetic field of 50 kOe was applied for 10 min and then removed. The data was collected raising the temperature at 2 K/min.

The curve presented in Fig. 7 can be fitted as follows:

$$M(0) = M_R \left(1 - \frac{T}{T_C} \right) \qquad (7)$$

where $M_R = 0.88 \times 10^{-3}$ emu g^{-1} and $T_C = (616 \pm 4)$ K. The critical temperature (T_C), which is high enough to propose the existence of strong interaction between the magnetic moments. For a common 3D ferromagnetic phase the equation follows a $T^{3/2}$

dependence law. In the present, the change in the exponent of T means that the ferromagnetic behavior is a bidimensional one [28]. Therefore, the observed $M \times T$ behavior could be related to the low dimensional structure of the material. Indeed, the polymeric backbone is a one-dimensional structure. However, it is important to stress that the ferromagnetic fingerprint was only observed in pressed pellets, indicating again that perpendicular interactions could have an important role in these systems.

4. Conclusions and final remarks

In summary, we concluded that the samples of poly(3-hexylthiophene) present different magnetic behaviors: diamagnetism, paramagnetism, and ferromagnetism. The results point that interchain interaction plays a significant role in the collective interaction of magnetic moments. Although the dipolar interaction is responsible for the ferromagnetic interaction in various polymeric systems [26,27], the intensity of this interaction is very weak and therefore could not explain the interactions at room temperature observed in the samples presented here. Thus, this type of interaction has been excluded as responsible for the interaction of the polymer. The critical temperature (T_C) obtained from spontaneous magnetization curve, around 616 K, showed that the interaction between the magnetic moments is strong. Finally, it has been demonstrated that when the samples are prepared under special conditions – like being in a partially reduced state – it leads to a concentration of polarons that allows the emergence of the ferromagnetic interaction. Optimizing this condition is an important goal to enable future applications of these materials as organic magnets in organic electronics.

References

[1] J.H. Burroughes, D.D.C. Bradley, A.R. Brown, R.N. Marks, K. Mackay, R.H. Friend, P.L. Burns, A.B. Holmes, Nature 347 (6293) (1990) 539–541.
[2] S.R. Forrest, Nature 428 (6986) (2004) 911–918.
[3] F. Garnier, R. Hajlaoui, A. Yassar, P. Srivastava, Science 265 (5179) (1994) 1684–1686.
[4] J. Janata, M. Josowicz, Nat. Mater. 2 (1) (2003) 19–24.
[5] W.H. Meyer, Adv. Mater. 10 (6) (1998) 439–448.
[6] M. Kuwabara, Y. Shimoi, S. Abe, Synth. Met. 101 (1999) 395–396.
[7] H.M. McConnell, J. Chem. Phys. 39 (7) (1963) 1910.
[8] H. Fukutome, A. Takahashi, M. Ozaki, Chem. Phys. Lett. 133 (1) (1987) 34–38.
[9] H. Murata, D. Miyajima, H. Nishide, Macromolecules 39 (2006) 6331.
[10] K. Yoshizawa, K. Tanaka, T. Yamabe, J. Yamauchi, J. Chem. Phys. 96 (7) (1992) 5516–5522.
[11] J.N. Devine, J.A. Crayston, J.C. Walton, Synth. Metals 103 (1-3) (1999) 2294–2295.
[12] A.A. Correa, L. Walmsley, L.O.S. Bulhes, W.A. Ortiz, A.J.A. de Oliveira, E. C. Pereira, Synth. Metals 121 (1-3) (2001) 1836–1837.
[13] F.R. de Paula, L. Walmsley, E.C. Pereira, A.J.A. de Oliveira, J. Magn. Magn. Mater. 320 (14) (2008) E193–E195.

[14] E.C. Pereira, A.A. Correa, L.O.S. Bulhues, P.C. Aleixo, J.A. Nóbrega, A.J.A. de Oliveira, W.A. Ortiz, L. Walmsley, J. Magn. Magn. Mater. 226 (2001) 2023–2025.
[15] O.R. Nascimento, A.J.A. de Oliveira, A.A. Correa, L.O.S. Bulhues, E.C. Pereira, V.M. Souza, L. Walmsley, Phys. Rev. B 67 (14) (2003) 144422.
[16] O.R. Nascimento, A.J.A. de Oliveira, E.C. Pereira, A.A. Correa, L. Walmsley, J. Phys. Condens. Matter 20 (3) (2008) 035214.
[17] F.R. de Paula, E.C. Pereira, A.J.A. de Oliveira, J. Supercond. Novel Magn. 23 (1) (2010) 127–129.
[18] S. Vandeleene, M. Jivanescu, A. Stesmans, J. Cuppens, M.J. Van Bael, H. Yamada, N. Sato, T. Verbiest, G. Koeckelberghs, Macromolecules 43 (6) (2010) 2910–2915.
[19] S. Vandeleene, M. Jivanescu, A. Stesmans, J. Cuppens, J. Van Bael, T. Verbiest, G. Koeckelberghs, Macromolecules 44 (2011) 4911.
[20] Z. Gulácsi, A. Kampf, D. Vollhardt, Phys. Rev. Lett. 105 (2010) 266403.
[21] G. Čik, L. Dlháň, F. Šeršeň, T. Pleceník, I. Červeň, Synth. Metals 159 (2009) 613–618.
[22] H. Nalwa, in: H.S. Nalwa (Ed.), Handbook of Organic Conductive Molecules and Polymers, vol. 3, 1st ed., John Wiley & Sons Ltd., New York, USA, 1997.
[23] N.C. Billingham, P.D. Calvert, P.J.S. Foot, F. Mohammad, Polym. Degrad. Stab. 19 (4) (1987) 323–341.
[24] F. Cataldo, M. Omastova, Polym. Degrad. Stab. 82 (3) (2003) 487–495.
[26] J. Roncali, Chem. Rev. 92 (4) (1992) 711–738.
[27] J.S. Miller, A.J. Epstein, Angew. Chemie-Int. Ed. English 33 (4) (1994) 385–415.
[28] C. Kittel, Introduction of Solid State Physics, 7th ed., Wiley India Private Limited, New Delhi, India, 2007.